Physica D 56 (1992) 406–429
North-Holland

PHYSICA D

Homeochaos: dynamic stability of a symbiotic network with population dynamics and evolving mutation rates

Kunihiko Kaneko[1]
Department of Pure and Applied Sciences, College of Arts and Sciences, University of Tokyo, Komaba, Meguro-ku, Tokyo 153, Japan

and

Takashi Ikegami[2]
The Graduate School of Science and Technology, Kobe University, Rokkodai, Nada-ku, Kobe 657, Japan

Received 10 May 1991
Revised manuscript received 2 February 1992
Accepted 3 February 1992
Communicated by A.V. Holden

Evolution of mutation rates is studied, in a population model with mutation of species coded by bit sequences and mutation of mutation rates. Even without interaction among species, the mutation rate is initially enhanced to search for fitted species and then is lowered towards zero. This enhancement opens a possibility of automatic simulated annealing. With the interaction among species (hosts versus parasites), high mutation rates are sustained. The rates go up with the interaction strength abruptly if the fitness landscape is rugged. A large cluster of species, connected by mutation, is formed by a sustained high mutation rate. With the formation of this symbiotic network resolved is the paradox of mutation rates: paradox on the stability of a rule to change itself. Population dynamics of each species shows high-dimensional chaos with small positive Lyapunov exponents. Stability of our symbiotic network is dynamically sustained through this weak high-dimensional chaos, termed "homeochaos".

1. Introduction

A mutation rate can change itself through evolution. We can think of various mechanisms to regulate the mutation rate [1]. The best known example is the proof-reading mechanism [2]. In the process of replication of DNA, differences between the original and its copy are detected and the errors are corrected. This proof-reading mechanism is widely found in living species and must have been developed in the course of evolution. In principle, the mutation rate can be decreased by elaborating the proof-reading mechanism.

In the present paper we study the evolution of a mutation rate. It is often erroneously believed that the evolutionary process always selects a lower mutation rate, and that the reason for the existing large mutation rate is just the overload of proof-reading. In other words, a more accurate proof-reading

[1]E-mail address: chaos@tansei.cc.u-tokyo.ac.jp.
[2]E-mail address: ikegami@gradis.scitec.kobe-u.ac.jp.

mechanism requires a longer time for replication, which leads to a lower rate of replication. The existing mutation rate could be determined through the balance of an intrinsic tendency to lower the mutation rate and the overload of proof-reading.

This argument is true for the evolution in fixed environment, but not necessarily so in a fluctuating environment or in a system where there is interaction among species. For example, both immune systems and viruses change their phenotype to adapt the interaction with each other, by adopting a strategy to enhance their mutation rates.

In the present paper we discuss the evolution of mutation rates, focusing on the mechanisms that sustain a high mutation rate through interactions among species (typically host vs. parasite, prey versus predator or host versus virus, or immune system versus virus, and so on)[#1].

This problem of evolution of mutation rates is important not only in biology, but also in physics and the genetic algorithm [5]. In the genetic algorithm, bit strings with messages are subject to evolution dynamics with mutation and splicing, where one has to control the mutation rate in advance. In a problem of optimization, simulated annealing has been developed as a powerful method, where the temperature for the Monte Carlo simulation is slowly cooled down according to a schedule fixed in advance. The temperature here plays the same role as the mutation rate, since both give an error rate of replication of a bit string. Our evolutionary dynamics gives a spontaneous change of mutation rates. Indeed we shall demonstrate that our evolutionary dynamics gives a spontaneous simulated annealing method. Even without an explicit interaction among species, the mutation rate in our dynamics is initially enhanced, leading to a global search for an optimized solution (fitted species). Once such a solution (species) is produced, the mutation rate is lowered automatically, leading to the increase of the population ratio of such species. Our dynamics of mutation rates leads to an innovation in genetic algorithm and simulated annealing.

Biological background

1. Proof-reading mechanism: In DNA replication, an enzyme reads base sequences and corrects them by removing wrong bases. This mechanism enhances the accuracy of DNA replication over 10^2 to 10^3 fold [1]. There can be various levels of proof-reading, leading to a control of mutation rates [2]. Thus mutation rates are not given, fixed numbers, but are themselves variable by mutation.

2. Immune system: A mutation rate in an immune system is enhanced to increase the diversity of antibodies, which face with an unknown antigenetic site [6]. The proof-reading mechanism may be operationally broken in a B cell as is reported by Rajewsky and his group [7]. This high mutation rate may look natural as for the level of a whole immune system. However, each antibody itself is a replicating unit. Many antibody species compete with each other for replication. Darwinian selection acts for each antibody.

If a state with a high mutation rate is sustained, however, it leads to a paradox, similar to the "self-referential paradox" [8]. Let us consider the following rule:

"*Rule*: *This rule should be changed*".

[#1] The evolution of recombination rate or the origin of sex is studied in connection with interaction with parasites. See e.g., ref. [3].

During the completion of the manuscript the authors have been informed of ref. [4], where the evolution of mutation rate is discussed in connection with the interaction of species. Although some of our motivation are common with theirs, the modelling and the point of view on the mechanism of high mutation rate are different.

As one can easily see, this rule has a paradox with self-reference, if the rule itself remains unchanged. One simple way to avoid the paradox is to change the above rule from "*should*" to "*should not*".

A state with a high mutation rate is subject to the above paradox. The above simple solution, of course, means decreasing the mutation rate towards zero. As will be seen, a high mutation rate, however, can be sustained throughout the course of evolution. Here we study how evolutionary systems find a way to live with the paradox, by introducing a model population dynamics.

Mathematically, a self-referential paradox is resolved without its removal by climbing up to a "meta" level, as has been clarified in Gödel's theorem [8, 9]. In the present paper we present an example in which the dynamics automatically leads to a meta-level description. Borrowing from the terminology of the dialectics, we may call this kind of dynamics "sublation dynamics".

In our model of the evolution, the original level is the survival of each individual species. The more identical offspring an individual reproduces that survives, the fitter it is in the evolution. Within the logical level of individual species, a sustained high mutation rate, i.e., a strategy to change itself, is a paradox. In our numerical results, the above paradox is resolved by a jump from the level of individuals to that of ensemble of species. Our system keeps the population in a network of species. In the level of ensemble of species, the rule to change the replication of each individual is no longer paradoxical. A high mutation rate in an immune system is also subject to the same paradox, since each antibody species is regarded as a self-replicating unit of a Darwinian system.

In the present paper we suggest that interaction of species may lead to a state with a high mutation rate. Generally speaking, there are three basic types of interactions among species; (1) host–parasite (or prey–predator) (2) cooperation, and (3) competition for a niche. In the first interaction type (host–parasite), one species gains through the interaction, while the other is damaged by it. In the cooperation, both species gain through the interaction, while both are damaged by the interaction in the competition. In the present paper we only consider the interactions (1) and (3). The inclusion of the cooperative interaction [10] to our studies is an interesting future problem, since recent studies suggest that the self-organization of the cooperative behavior depends strongly on mutation rates [11].

We assume that the inherent population dynamics of each host species is subject to the fitness landscape. In addition to the above interaction, the population change of each species depends on the fitness attached to it. The fitness is often thought to depend in a complex manner on the gene sequence, with many local hills and valleys. We study the dependence on the landscape also, using a spinglass model or flat (neutral) landscape.

The present paper is organized as follows. In section 2, our basic model is introduced, which consists of a population dynamics and a Monte Carlo algorithm for mutation[#2]. The dynamics includes the interaction among hosts and parasites, suppression of population due to the competition, and the natural growth or decay, depending on the fitness of each species. Section 3 is devoted to a simple case, evolution of mutation rates without interaction between species. As is expected, the mutation rate goes down finally, but a transient increase is often observed. The possible relevance to automatic simulated annealing is also discussed.

In section 4, the evolution of mutation rate is discussed with host–parasite interaction, where the mutation rate of the parasite is fixed. If the coupling is large, the mutation rate is sustained at a high level.

[#2] Throughout the present paper we focus only on point-mutation. By the term "mutation", we refer only to point-mutation. Any other mutation mechanisms are not discussed.

A mechanism of this sustained high mutation rate is attributed to the formation of an oscillatory network in section 5. In the mutation induced population dynamics, a non-zero population is preserved in a network, competing in a host–parasite interaction. We introduce a term "oscillatory symbiotic network" (*symbionet*), since all species coexist within the network. The oscillation turns out to be chaotic. The ensemble of species is maintained only through chaotic change of each population. Indeed, a fixed-point or periodic state is unstable. The final persistent state is sustained by chaos. This observation introduces a novel and important notion, *homeochaos* – see section 6. In homeochaos, the strong instability in low-dimensional chaos is smoothed out, and the dynamic stability is sustained in high-dimensional hyperchaos.

In section 7 we study dependence of mutation rates on the environmental landscape. If the evolution is neutral, a sustained high mutation rate is again observed, where the size of oscillatory network is large. In the neutral case, no sharp transition is observed. Up to section 7, the mutation rate of parasites is fixed. In section 8, we study a model in which both the mutation rates of hosts and parasites vary. Again, we find a state with high mutation rates for both species. Section 9 is devoted to discussion of our results in possible connection with real biological networks.

2. Modelling

We assume that there are host (prey) species and parasite (predator) species. Both species of hosts and parasites are coded by a bit string σ_i, whose length is fixed at k. In the paper we choose $k = 7$ unless otherwise mentioned. For example, the species 42 has a bit string 0101010. Each species is further classified with respect to its mutation rate, so that it is coded by two variables. We denote each species by (i, j), whose population is given by $h(i, j)$ and $p(i, j)$, for a host and a parasite, respectively. Here i is a k bit word defining the species, while j is the mutation level. Our evolutionary dynamics thus consists of the population of $h(i, j)$ and $p(i, j)$. Possible mutation rates are discretized into 13 levels, in an exponential scale. The mutation rate of the species (i, j) is given by $\mu_j = 2^{j-13}$ $(j = 1, \ldots, 13)$[#3].

Introducing an ensemble of species, we carry out the following processes for the evolutionary dynamics:

(i) mutation: $\{\sigma_1, \sigma_2, \ldots, \sigma_j, \ldots, \sigma_7\} \to \{\sigma_1, \sigma_2, \ldots, 1 - \sigma_j, \ldots, \sigma_7\}$. Here we assume that there occurs at most only a single-point mutation for each sequence. The rate of this single-point mutation error is given by its mutation rate μ_j.

(ii) mutation of mutation rates: We assume that the mutation rate $(\mathrm{d}\mu_j/\mathrm{d}t)$ of mutation rate (μ_j) is also controlled by the same mutation rate (μ_j) itself. This is the source of self-referential paradox. At each step, a mutation rate can mutate either upwards or downwards with equal probability. Practically we adopt the following algorithm; take a random number $r \in [0, 1]$. If r is larger than $1 - \mu$ the mutation from the species (i, j) to $(i, j + 1)$ occurs, while that from (i, j) to $(i, j - 1)$ occurs, if r is less than μ. (At $j = 13$ or 1, only downward or upward mutation occurs, respectively.)

(iii) Host–parasite interaction: The interaction between hosts and parasites is of the Lotka–Volttera type, which, we assume, is given by a function of the Hamming distance between their bit strings. As the simplest coupling between a host and a parasite, we adopt a perfect matching. Only a parasite with the

[#3] There is no explicit reason that the mutation rate should be in an exponential scale. For example, we assume that the mutation level j codes the number of times of proof-reading, and each proof-reading reduces the error rate to half.

same bit string as a host exploits the host. The population of the host is decreased by the interaction while that of the parasite is increased.

(iv) Reproduction or death (in a flat or rugged landscape): Besides the interaction among species, different species may have different fitness generically. If the evolution is neutral [12], the fitness function is flat (constant) for all species. Generally the fitness depends on the genetic sequence in a complex manner. If the fitness is plotted as a function of the sequence, the landscape there may have many hills and valleys, as is often called rugged landscape. In the present paper we treat only the following two cases: (a) both the mutations of hosts and parasites are neutral. The fitness landscape is flat. (b) mutation of parasites is neutral, but that of hosts is not. The fitness for hosts have "rugged landscape" [13].

In a rugged landscape, the fitness has a complex dependence on the genetic sequence (bit string). A spinglass model gives a simple example for such a rugged landscape. In a spinglass, energy is assigned to a binary sequence $[\sigma_i]$. A typical model is the Sherrington–Kirkpatrick (SK) model [14]. In this model the energy is given by $E = \sum J_{i,j} S_i S_j$, where $S_i = 2\sigma_i - 1$ takes 1 or -1, and $J_{i,j}$ is a fixed random value distributed over positive and negative values. We take the distribution to be homogeneous over $[-\gamma, \gamma]$. The model is known to provide many metastable states in a rugged landscape [14]. As the parameter γ is increased, the height of hills and valleys increases, leading to the increase of ruggedness. We use the SK model for the fitness function; fitness is given by $\exp[E_0 - E(i)]$ [15, 16]. A species with lower "energy" has higher fitness. For a neutral case we take $E(i) \equiv 0$ for all species.

For parasites, we assume that the fitness function is intrinsically neutral. Only the host–parasite interaction term depends on species. Including the natural death, the population at the next step decays by a factor d with $d < 1$.

(v) Competition among individuals: There is strong competition within same species or in a group of species with the same niche. Indeed, this interaction suppresses the divergence of population in most models, such as in the nonlinear term in Verhulst–Malthus equation ($dx/dt = ax - bx^2$).

In the present paper we choose the following two types of suppression. For parasites we assume the first suppression type (type-I), competition only within the same species: this effect is introduced through the suppression term $1/[1 + g\sum_j p(i,j)]$ in the population dynamics. The term reduces the population when the total population outgrows (e.g. $\sum_j p(i,j) \gtrsim (1/g)$). Since all species with same bit string have the same phenotype, without respect to its mutation level j, the above summation over a whole mutation level is required.

The other case (suppression-type-II) is used for the suppression of hosts; the competition within all species. In other words, all species compete for the same niche. By taking the same type of coupling as the first case, we choose the suppression term $h(i,j)/[1 + g\sum_{i,j} h(i,j)]$ here. If the total population is larger than $1/g$, the suppression is effective.

Combining (i)–(v), the population dynamics consists of successive operations of the mutation algorithm $[p_n(i,j), h_n(i,j)] \to [p''(i,j), h''(i,j)]$ and then the following dynamics:

$$h_{n+1}(i,j) = \mathrm{Int}\left\{\left(\exp[E_0 - E(i)] - c_h \sum_k p''(i,k)\right) h''(i,j) \Big/ \left(1 + g_h \sum_{i,k} h''(i,k)\right)\right\}, \tag{1}$$

$$p_{n+1}(i,j) = \mathrm{Int}\left\{\left(d + c_p \sum_k h''(i,k)\right) p''(i,j) \Big/ \left(1 + g_p \sum_k p''(i,k)\right)\right\}, \tag{2}$$

where $\mathrm{Int}\{\ldots\}$ is the integer part of $\{\ldots\}$. This completes the dynamics $[p_n(i,j), h_n(i,j)] \to$

$[p_{n+1}(i,j), h_{n+1}(i,j)]$. Starting from an ensemble of species, we first apply the mutation algorithm for the population of hosts and parasites using Monte Carlo methods, to get the intermediate population p'' and h''. The populations at the next time step are given by eqs. (1) and (2). This completes the first time step. We continue these procedures for many time steps.

Initial condition: We typically choose either of the following two initial conditions. (1) only one or two species of hosts and parasites with matched strings have non-zero population. (2) Many host and parasite pairs have equal non-zero population. We mostly assume that initial mutation levels are concentrated on a single level.

As far as we have checked, the initial condition dependence is not crucial. Basins of attraction for states which we show in later sections are rather large. Attractors do not seem to be unique, but for most macroscopic quantities such as the final mutation level or the total population, initial condition dependence is rather small, in so far as we have seen, as long as our system does not go to a state of "extinction".

Indeed, for some parameters or for some initial conditions, global extinction of all hosts or parasites may occur. This extinction state itself is stable. There is no creation of species from the extinct state, of course. We believe that possible extinction is a feature of natural evolutionary system, but it is not included in most other evolutionary models [3, 4], where the total population is often kept constant.

3. Evolution of mutation rates without interaction between host–parasites

Before starting to describe our main results, let us briefly survey simulations without host–parasite interactions.

In fig. 1, temporal change of average mutation level is plotted for a system without any parasites. As has been expected, the mutation rate ultimately goes down with time. Once a species with a higher fitness is selected, species with lower mutation rates have more offspring, independent of the population distribution, since the population dynamics of one species does not directly depend on the population of the other species. This argument is true after the species finds a string with a high fitness in the landscape. In the transient time, the mutation rate can increase, if the initial ensemble does not include species of high fitness (see fig. 1). After the transient, the mutation rate decreases towards zero.

The above transient increase of mutation rates is easily explained. Species with higher mutation rates are faster in the search for larger fitness. Once the species with large fitness appears, it is then better to have a strategy to reproduce the species with a smaller error. Their mutation rate starts decreasing.

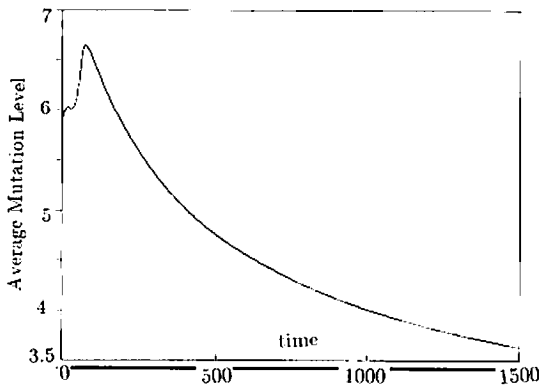

Fig. 1. Temporal change of average mutation level of host species without parasites. Initially a single species ("19" with mutation level 7) is put. $E_0 = 0$, $\gamma = 1.0$, and $g_h = 0.0001$. Other parameters are not required since there are no parasites.

Although the above example is rather simple, this mutation of mutation rate opens a possibility of automatic simulated annealing. In the conventional simulated annealing [17], one has to change the temperature ("mutation rate") externally. Initially the system should be put in a high temperature, to search effectively for many local minima, and then the temperature is lowered externally as the system finds a configuration with lower energy. In the simulated annealing, one has to give a schedule of temperature decrease in advance, which depends on a problem to optimize.

Our algorithm with mutation of mutation rates automatically enhances a mutation rate initially and then lowers it as the system finds a lower energy. During the time steps with enhanced mutation rates, lower energy is globally searched for, while the mutation is decreased once a species of very low energy is found. Thus one can reach optimal sequences very effectively, with this inclusion of mutation of mutation rates. We note that our algorithm does not require any external change of mutation (temperature) rates. Everything goes spontaneously, once an initial condition is given. Our model dynamics can provide a novel algorithm, by which the conventional simulated annealing may be replaced [18].

The use of evolution in optimization problems is popular now, as genetic algorithms [5]. In a genetic algorithm, mutation rates are usually fixed. Our example shows that the inclusion of mutation of mutation rates gives an innovation in genetic algorithm, compiling with the automatic simulated annealing.

4. Maintenance of a high mutation rate through the interaction among species

For the following four sections, we assume that the mutation rate of parasites is fixed at μ_p. Only a mutation rate of a host is variable by mutation. The main control parameters in our model are μ_p, c_p and c_h. Fig. 2 gives an example of temporal evolution of the averaged mutation rate for host species. If the couplings c_p and c_h are large enough, the average mutation level suddenly climbs up to a higher value, and it is stably sustained afterwards. The level often overshoots as in fig. 2a, and then is lowered down to the final value. When an initial mutation level is too large, the level monotonically decreases down to the (same) final level and stays there. On the other hand, the average mutation rate gradually decreases towards zero if the couplings are weak.

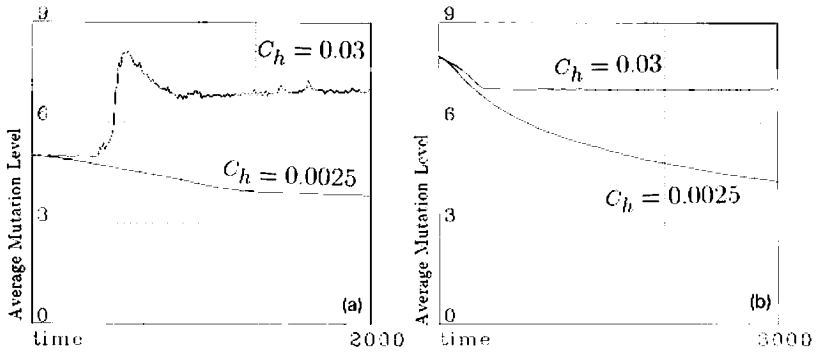

Fig. 2. Temporal change of average mutation level of host species. Initially a single species (19 with mutation level 7) is put. $g_h = 0.0001$, $g_p = 0.1$, $c_p = 0.008$, $d = 0.9$, $\mu_p = 0.05$. (a) neutral case ($E_0 = 0.5$, $\gamma = 0$). (b) rugged landscape ($E_0 = 0.4$, $\gamma = 0.2$).

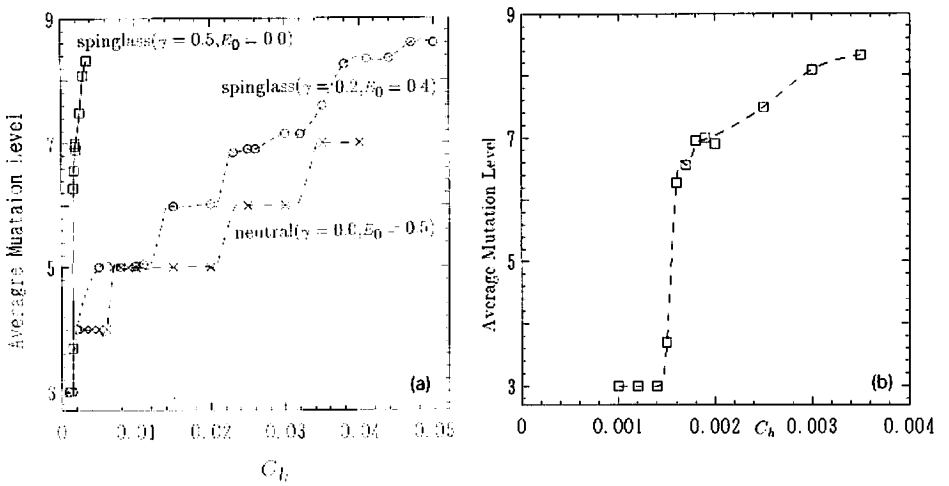

Fig. 3. Final average mutation level plotted as a function of c_h. Initially a single species (19 with mutation level 7) is put. $g_h = 0.0001$, $g_p = 0.01$, $c_p = 0.008$, $d = 0.9$, $\mu_p = 0.05$. (a) □ ($E_0 = 0.0$, $\gamma = 0.5$), ○ ($E_0 = 0.4$, $\gamma = 0.2$), × (neutral, $E_0 = 0.5$, $\gamma = 0$). (b) expansion of (a).

Dependence of final mutation level on couplings is shown in fig. 3. Here we change the strength of coupling (c_h), damage of a host by the parasite of the same bit sequence. The mutation level increases in a stepwise way with the coupling strength. As a host is damaged more by a parasite, the mutation level is lifted up to a higher value. On the other hand, the final mutation level of hosts depends more weakly on the mutation rate of parasites.

The sustained mutation rate depends on the landscape. As the valley height γ is increased in the landscape, the transition gets sharper (fig. 3). In a flat landscape (neutral evolution $\gamma = 0$), the transition is smooth and consists of successive steps, as will be discussed in section 7.

Temporal changes of populations of species are remarkably different in the low and high coupling regimes. For the low coupling regime with decreasing mutation rates, the population dynamics approaches a fixed point with small fluctuation. This small fluctuation originates in the stochastic nature of mutation. Besides this fluctuation, a fixed landscape is attained through evolution, which is consistent with decreasing mutation rates. If the mutation rate is small enough, the dynamics of each species i is essentially separated from other species j. Then the dynamics here is governed by the following globally coupled two-dimensional map:

$$h_{n+1}(i) = \left[\alpha(i) - c_h p_n(i)\right] h_n(i) \Big/ \Big(1 + g_h \sum_i h_n(i)\Big), \tag{3}$$

$$p_{n+1}(i) = \left[d + c_p h_n(i)\right] p_n(i) \Big/ \left[1 + g_p p(i)\right], \tag{4}$$

where $\alpha(i) = \exp[E_0 - E(i)]$. The fixed point of the above map is given by $p(i)^* = (\langle\alpha\rangle - 1)c_p - (1-d)g_h'/(c_p c_h + g_p g_h') + (\alpha(i) - \langle\alpha\rangle)/c_h$ and $h(i)^* = (1-d)/c_p + g_p p(i)^*/c_p$ which is unstable under the following condition (see appendix):

$$c_h > g_p(2 - \langle\alpha\rangle)/2(1-d)\left[1 + \sqrt{1 + 4(1-d)g_h'/c_p(2-\langle\alpha\rangle)^2}\right], \tag{5}$$

where $\langle\alpha\rangle$ is the average growth rate given by $\langle\alpha\rangle = \Sigma_i \exp[E_0 - E(i)]/\Sigma_i 1$. This inequality states that

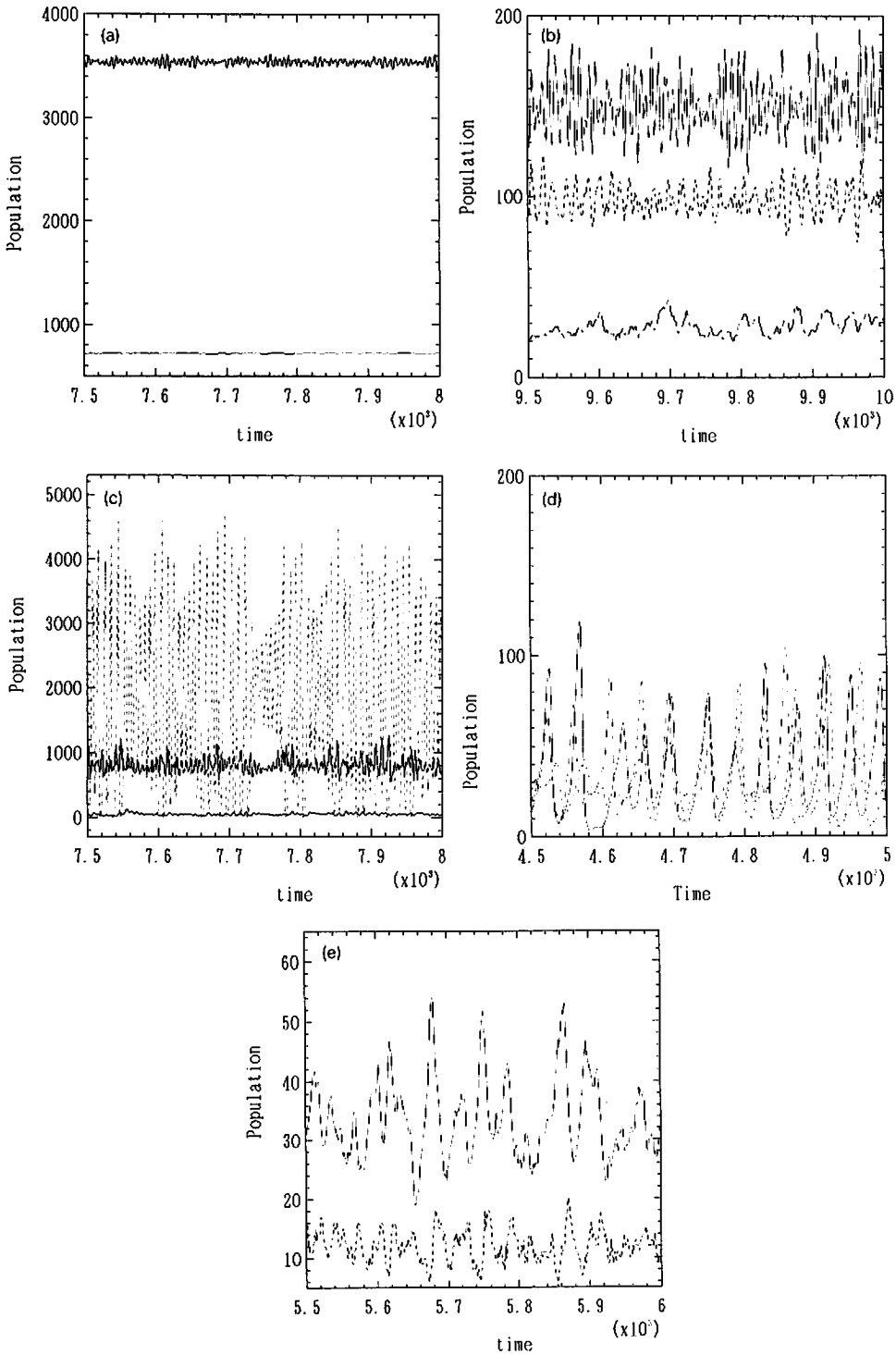

Fig. 4. Temporal change of population of some species. $g_h = 0.0001$, $g_p = 0.01$, $c_p = 0.008$, $d = 0.9$, and $\mu_p = 0.05$. (a) $E_0 = 0.4$, $\gamma = 0.2$, and $c_h = 0.002$, where final mutation level is still going down (around 3) for species 3 ($E_3 = -0.376$, bottom) and species 7 ($E_7 = -0.544$, top). (b) $E_0 = 0.4$, $\gamma = 0.2$, and $c_h = 0.012$, taking the same coupling $J_{i,j}$ with as (a). Population of species 3 (dotted line), 5 (broken line, $E_5 = -0.215$, bottom) 7 (solid line). $c_h = 0.1$. Final mutation level is around 5. (c) $E_0 = 0$, $\gamma = 0.5$, and $c_h = 0.002$. Population of species 3 (solid line, bottom $E_3 = -0.94$), 7 (solid line, around the middle, $E_7 = -1.36$) 19 (dotted line, $E_{19} = -1.80$). $E_0 = 0$, $\gamma = 0.5$, $c_h = 0.002$. Final mutation level is around 7. (d) population of species 1 (solid line), 2 (broken line), and 3 (dotted line). Neutral case ($E_0 = 0.5$, $\gamma = 0$, and $c_h = 0.015$). (e) Population of host species 1 (solid line) and corresponding parasite (dotted line). Parameters are the same as in (d).

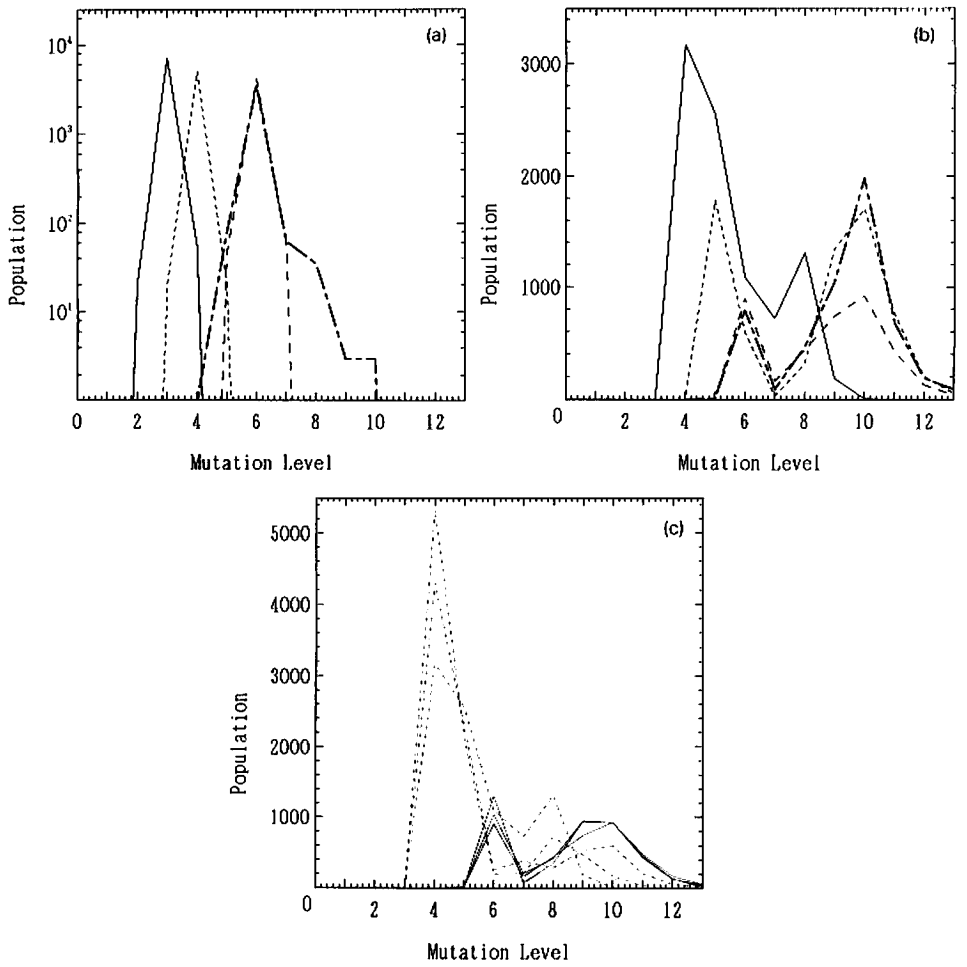

Fig. 5. Distribution of average mutation level: Histogram of population for each mutation level (irrespective of species) is plotted. The histogram is the accumulation of population over 8000–10000 time steps. $g_h = 0.0001$, $g_p = 0.01$, $\mu_p = 0.05$, and $c_p = 0.008$. (a) $\gamma = 0.2$, $E_0 = 0.4$. $c_h = 0.005$ (solid line). $c_h = 0.01$ (dotted line), $c_h = 0.015$ (broken line), and $c_h = 0.02$ (thick dotted broken line). (b) $\gamma = 0.4$, $E_0 = 0$. $c_h = 0.003$, (solid line), $c_h = 0.008$ (dotted line), $c_h = 0.013$ (broken line), and $c_h = 0.018$ (thick dotted broken line). (c) same parameter as (b) for γ and E_0. Starting from three sets of initial conditions, the first for initial species 19 only, the second for 19 and 39, and the third for 19, 39, 59, 79, 99, and 119. $c_h = 0.003$ (dotted line), and $c_h = 0.013$ (solid line).

the fixed point is unstable in the strong coupling regime, as is consistent with our observation. For the sustained mutation state, the population of hosts and parasites oscillates in time. At the onset parameter of this state, this oscillation is very weak, although it is aperiodic. As the coupling is increased, the amplitude of the aperiodic oscillation increases.

Mutation levels are not necessarily the same within an entire species. When the average mutation level is low (or going down), the distribution of mutation level is concentrated on its average. The mutation level is restructed to almost a single level for species with large enough population. If the valley height of energy is not high, the distribution of mutation level is again rather sharp for each species, if the coupling is not too large (see fig. 5a). The distribution is concentrated on a single level, with very little spreading to the neighboring levels. As the valley height of landscape is increased, the distribution gets broader. If the final state has a larger mutation rate with large fluctuation, the mutation level differs by species.

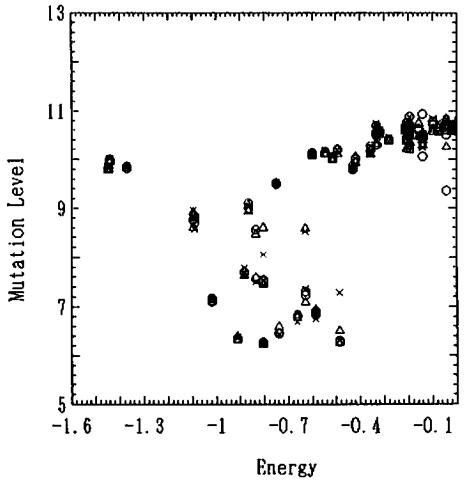

Fig. 6. Average mutation level as a function of energy of species. Same parameters as fig. 5b are chosen, with $c_h = 0.018$. Data $\triangle$ are from the initial condition with species "19" only, $\times$ from species "19" and "39", and $\circ$ from "19", "39", "59", "79", "99", and "119".

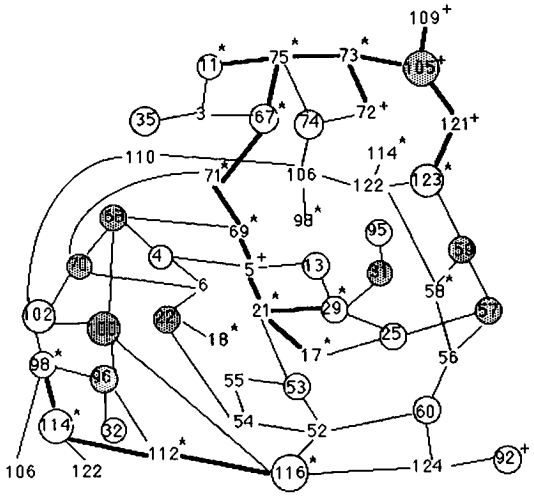

Fig. 7. Connection of species by single point mutation: species satisfying the following two conditions are depicted as nodes of the graph: (1) Its energy is lower than -0.5. (2) It never extincts during the time step from 800 to 1200. The mutation rate of each species is computed by averaging over the time steps from 800 to 1200 under the parameters of $\gamma = 0.2$, $E_0 = 0.4$, $c_h = 0.03$. In the graph, two nodes are connected only if their Hamming distance is equal to 1. Species with low mutation rates, denoted by asterisks (rates less than 2^{-7}) and by crosses (between 2^{-6} and 2^{-7}), turn out to form an almost linear chain among the sea of the species with higher mutation rates. (This chain connection is shown as a thick bond). In the graph, species within a dark cycle have energies less than -0.8 and those within a white cycle have larger energies than -0.6.

When the valley height of landscape is high (i.e., the ruggedness of landscape is strong), the distribution of mutation levels has two peaks as is seen in fig. 5b. Different species split into two groups with distinct mutation levels. As the coupling c_h is increased, the peak at the higher level gets larger. Although the distribution slightly depends on initial conditions, its main structures, such as the number of peaks and their position are invariant with the choice of initial conditions, as is seen in fig. 5c.

The average mutation level is plotted as a function of energy of species in fig. 6, when the distribution has two peaks[#4]. Some species have high mutation rates, while others have lower ones. One can see the tendency of increasing of the mutation level both at a smaller energy and a larger energy[#5]. The latter increase is due to "unstable" species which exist only as paths between metastable species. A higher mutation rate of species with a small energy results from these oscillations in its population. Since the increase rate $\exp[E_0 - E(i)]$ is large enough to lead to an increase of parasites, the species would become

[#4] When there is only a single peak for the distribution of mutation (in a weak coupling regime), the plot corresponding to fig. 6 is almost flat, although there is again a weak tendency of increase of a mutation level both at larger and smaller energies.

[#5] In figs. 6 and 8, we have plotted only the data with $E(i) < 0$. There are some species for positive energy, whose population, however, is very small and exists only through rare mutation.

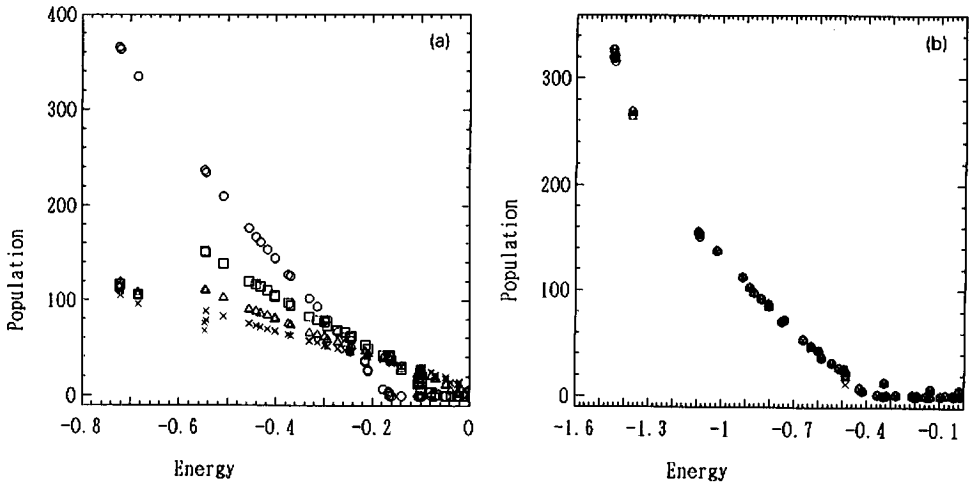

Fig. 8. Average population of species as a function of energy of species, corresponding to fig. 5a and fig. 6b, respectively. (a) $\gamma = 0.2$, $E_0 = 0.4$. $c_h = 0.005$ (○), $c_h = 0.01$ (□), $c_h = 0.015$ (△), and $c_h = 0.02$ (×). (b) Data △ are from the initial condition with species "19" only, × from species "19" and "39", and ○ from "19", "39", "59", "79", "99", and "119".

extinct by the attack of parasites, if there was no mutation. The large mutation at a small energy comes from this strong (chaotic) oscillation. This observation leads to the picture of oscillatory network in the following section. Among species with middle energy, there are some groups of species with a much lower mutation level. These groups form a chain circuit of species connected by mutation (see fig. 7 for a connection network by mutation).

For comparison, the average population is plotted in fig. 8. The population increases roughly linearly with $E_c - E(i)$ from a threshold E_c, except at very low energy. For very small energy, it is deviated to a lower population if the landscape is too rugged.

5. Formation of oscillatory symbiotic network

By what mechanism is a high mutation rate maintained? First, we recall the dynamics of population of each species. For the sustained state with a high mutation rate, the populations of hosts and parasites oscillate in time. Through the host–parasite interaction, host species i with large population is largely exploited by the parasite species i. Then the population of parasite i increases, leading to the decrease of that of host i. Through the mutation, there is flow of population from species i to other species. There remain some populations in the species reached by a single point mutation from this damaged species i, even if the attack by the parasite is very strong. After the population of host i is largely decreased, that of parasite i starts to decrease, since the gain term $\Sigma h(i, j)\, p(i)$ from the interaction gets very small. After this decrease of population of parasite i, flow to the host i through mutation raises the population of host i. This oscillatory scenario is possible only if the mutation rate is not too small.

5.1. Oscillation network

In a Darwinian selection system, we naively tend to believe that it is a better strategy to have more offspring with the same gene sequence. However, with the interaction among species, this strategy is not

necessarily possible in the level of each individual species. Instead of being kept in each species, the population is kept in an ensemble of species, connected as a network through mutation. In other words, the system assumes a higher logical type (meta-level), from individual species to network of species. This formation of an oscillatory network resolves the self-referential paradox without erasing it.

Host species coexist in this network. The existence of other species is essential for the survival of each species. In this sense, we call the above network as symbiotic network, or *symbionet*, in short. The network is sustained through the oscillation among species. Connection through a network comes from successive population changes among species, due to mutation and host–parasite interactions.

5.2. *Percolative behavior*

In a strong coupling regime, the average mutation level increases rather abruptly when we start from a low mutation regime (see fig. 2a). After this temporal transition, a high mutation rate is stably sustained by the strong coupling. This transition shares a common feature with percolation phenomena. The sudden increase of mutation level is also seen with the change of coupling c_h, especially when the valley height (γ) of landscape is high (see fig. 3b). In order to check this percolative nature, we introduce the following "mutation cluster".

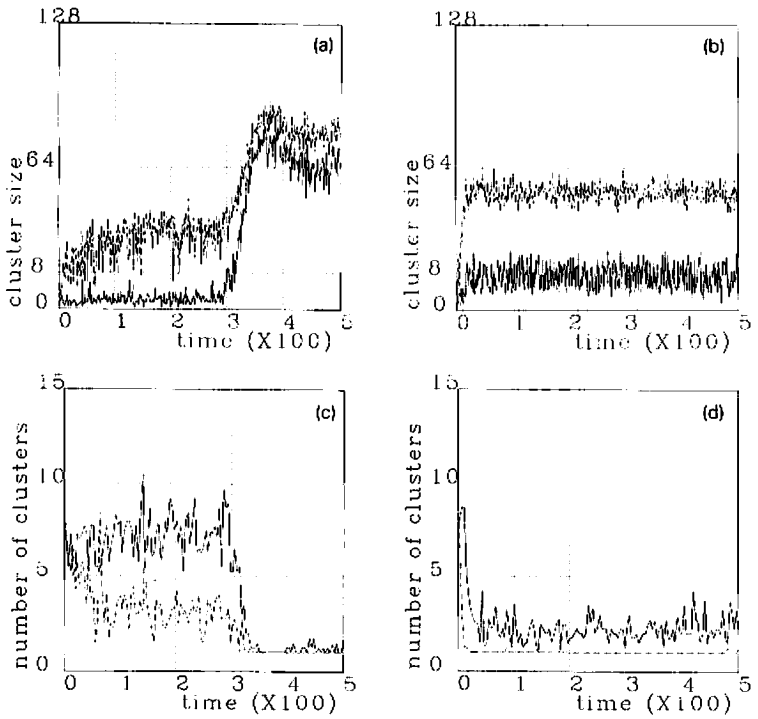

Fig. 9. Temporal change of maximal mutation cluster size (a, b) and corresponding change of the number of independent clusters (c, d) for hosts (solid lines) and parasites (broken lines). In (a) and (c) simulation is carried out with the parameters $\gamma = 0.2$, $E_0 = 0.4$, and $c_h = 0.03$, where an averaged mutation rate abruptly climbs up around 350 steps. Parameters for (b) and (d) are $\gamma = 0.2$, $E_0 = 0.4$, and $c_h = 0.0025$, where the mutation rate gradually decays. The increase of the maximal cluster size simultaneously occurs with that of the mutation rate. In (d), the number of clusters is not large, since few species survive.

A mutation cluster is defined as an ensemble of species connected by ongoing mutation. Since many possible species do not have any population, all existing species are not necessarily connected by mutation. Each species of a host–parasite pair may be isolated. Many disconnected clusters coexist, whose size is unity or very few. In a strong coupling regime, on the other hand, many species may be connected through mutation to form a large cluster, in which a high mutation rate is stably sustained by itself. A host damaged by a parasite is immediately compensated by other host species through mutation within the cluster.

In practice, we carry out the following procedure for a mutation cluster. First define a mutation flow from a species i by an actual event of population flow from the species. If there is at least a single event of mutation from the species i, it is defined as a node of a mutation cluster. A cluster by definition is "connected", i.e., every node of the cluster has its nearest species as a node (e.g. a species with a Hamming distance 1 from that node).

Before the transition to a high mutation regime, there are many independent clusters, members of which may change in time. Each cluster has very few (often a single) numbers of species. The average cluster size of network is close to unity in the low coupling regime. With time, the cluster size suddenly increases, accompanied by the transition to a high mutation rate. A large mutation cluster (network of species) is formed. At and after the transition, those independent clusters stick together, generating one big cluster. The size of cluster increases from $\mathcal{O}(1)$ to $\mathcal{O}(2^k)$, which also implies that the number of clusters decreases to $\mathcal{O}(1)$ (see fig. 9). Species connected by mutation are "percolated"[#6] in the whole bit space of 2^k species.

This formation of a large percolated cluster is also seen with the change of coupling. As the coupling is increased, the size of cluster increases from $\mathcal{O}(1)$ to $\mathcal{O}(2^k)$, while the number of clusters decreases to $\mathcal{O}(1)$. The transition is rather sharp, as is typical in percolative behavior.

6. Homeochaos

Let us focus on a dynamical aspect of the network in the present section. Before the transition to a high mutation rate, a few host–parasite pairs or a small set of few species form isolated nodes of clusters. Population dynamics of each independent cluster (e.g. a few degrees of freedom) can be chaotic. The total dynamics, then, is approximated by a direct product of independent low-dimensional (chaotic) dynamics of host–parasite pairs. On the other hand, population dynamics in the high mutation regime is essentially high-dimensional chaos, since all populations within the cluster are coupled, and the above direct-product picture is no longer valid.

Since the exact calculation of Lyapunov spectra including the mutation part is rather difficult, we compute, for simplicity, the eigenvalues of the product of Jacobi matrices of the population dynamics; that is, the Jacobian matrix for hosts and parasites (see appendix). From the eigenvalues of the product of the Jacobi matrices, one can obtain Lyapunov spectra which give a rough measure for the chaos.

In the weak coupling regime with decreasing mutation rate, Lyapunov exponents are broadly distributed. Some have very large positive exponents, while some others have negative ones, as are shown in fig. 10. This behavior is expected since the dynamics of each host–parasite pair is roughly separated

[#6] This kind of "percolation"-like behavior is often seen in network formation, as is discussed in the autocatalytic network, immune network, and so on.

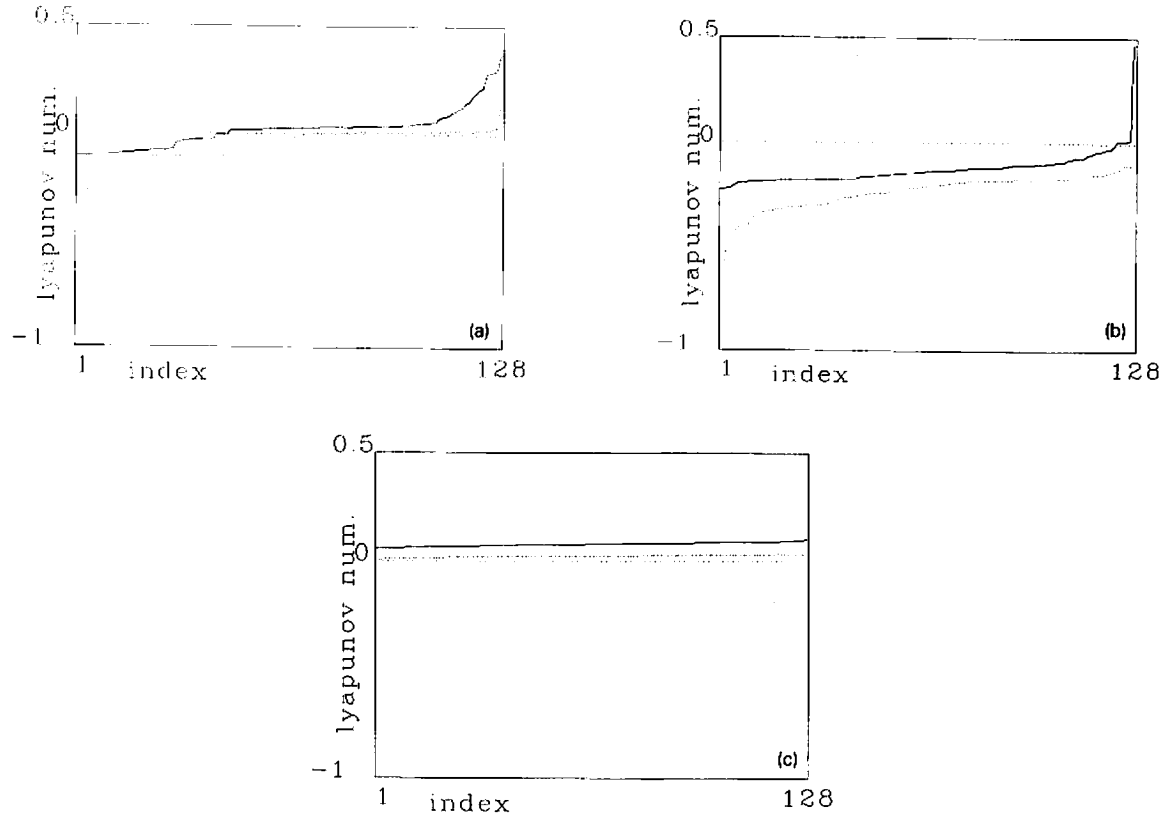

Fig. 10. Lyapunov spectra obtained by the method in the text after discarding initial transients (solid lines for hosts and broken lines for parasites). They are obtained through the products of Jacobi matrices for time steps from 4000 to 5000 (a), (c) and from 2000 to 3000 steps (b). Parameter for (a) and (b) are given by $\gamma = 0.2$, $E_0 = 0.4$, and $c_h = 0.03$ (a) or $c_h = 0.005$ (b). (c) is obtained for a neutral case with $E_0 = 0.4$ and $c_h = 0.03$.

(except the saturation term in the denominator), and dynamics of each two-dimensional map has a large variety ranging from strong chaos to a stable fixed point, depending on its energy $E(i)$.

In the strong coupling regime with a high mutation rate, the Lyapunov spectra have a plateau at a slightly positive value. By forming a large connected cluster, the system exhibits high-dimensional chaos. The exponents are concentrated on small positive values (see fig. 10). This observation confirms our view that the high mutation rate is sustained under weak chaotic oscillation. For the neutral landscape, we again have a plateau of positive exponents for a high mutation regime.

We have also studied the distribution of eigenvalues of the Jacobi matrix of the population dynamics for one time step[#7]. During the initial transients of evolution, eigenvalues are dispersed over 0.5 to 5. The amplitude of population oscillation is large reflecting the dispersed distribution. For the weak coupling regime, eigenvalues concentrate below 1 after initial transients; a fixed point solution of the system is stable. On the other hand, eigenvalues concentrate around (just above) unity for the strong coupling regime: A fixed point solution becomes unstable, but the instability is not so strong as in the

[#7]See appendix for analytical estimates of the eigenvalues around the Hopf bifurcation of the fixed point solution.

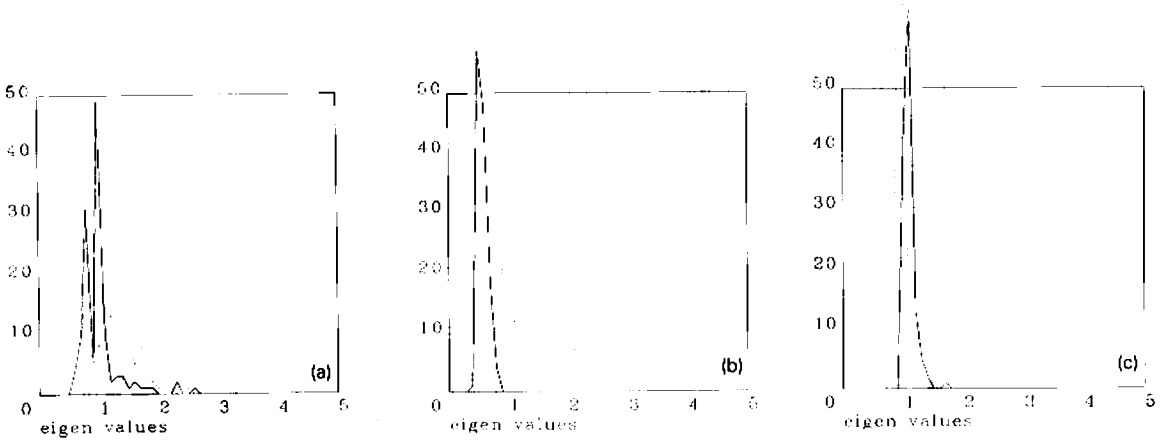

Fig. 11. Distribution of averaged eigenvalues of Jacobian matrix, which are computed from the first 100 steps and the last 100 steps after the mutation rates settle down to final values (a), (c), while we use the first 10 and last 10 steps for (b) since the convergence is rather rapid there. Parameters are chosen to be $\gamma = 0.2$, $E_0 = 0.4$, and $c_h = 0.03$ for (a); and $\gamma = 0.2$, $E_0 = 0.4$, and $c_h = 0.0025$ for (b). (c) uses a neutral landscape with $E_0 = 0.5$ and $c_h = 0.03$.

initial transients (see fig. 11). Also note two separated parts of the distribution of exponents (see fig. 11). This separation corresponds to the double peak distribution of mutation levels in section 4.

A weak chaotic motion suppresses the amplitude of the population oscillation. Although the oscillatory behavior is related with the formation of network, too large an oscillation may be fatal to our system, since many species may die out. Through the evolution of mutation rates there is a tendency of decrease in oscillation amplitude. If a cluster is small, each host is largely damaged by parasites. This kind of host–parasite (prey–predator) interaction leads to a large amplitude oscillation. Through the evolution of mutation rates, the cluster gets larger, and the number of species involved in this interaction increases, leading to the decrease of the amplitude of the population oscillation, as is clearly seen in fig. 12.

In short, our system has a tendency to evolve towards a state with weak chaos with a large number of degrees of freedom. In the term "weak", we mean that the maximum Lyapunov exponent is not so large,

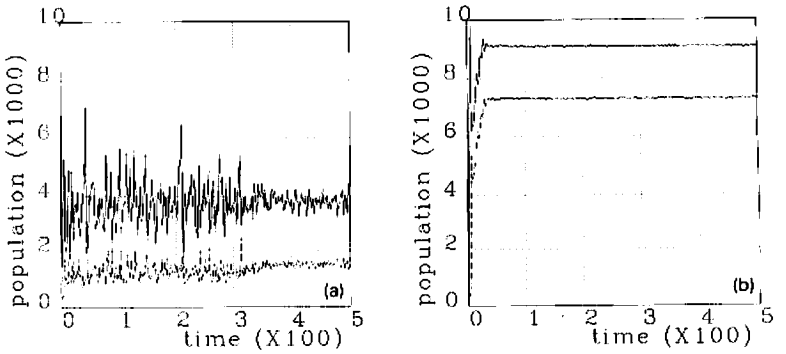

Fig. 12. Oscillation of total populations for hosts (solid line) and parasites (dashed line). (a) $\gamma = 0.2$, $E_0 = 0.4$, and $c_h = 0.03$; Initial chaotic oscillations with large amplitudes are suppressed simultaneously with an abrupt increase of averaged mutation rate around 320 time steps. (b) $\gamma = 0.2$, $E_0 = 0.4$, and $c_h = 0.0025$. The population dynamics approaches a fixed point with a gradual decay of mutation rates.

and that the amplitude of oscillation of each species is small. In the term "large number of degrees of freedom", we mean that the number of positive Lyapunov exponents is large. Chaotic modes are shared with many species connected by our symbionet.

It has often been discussed that the stability of population dynamics is lost with increasing number of species [19]. This argument does not hold for chaotic processes. Our result suggests that an evolutionary system with many species maintains its stability at a weak high-dimensional chaotic state, rather than in a fixed point or in strong chaos. We may call this homeodynamic[#8] state as homeochaos.

As a working hypothesis of homeochaos, we stress the following three points:

(i) Dynamic stability. Homeochaos provides a dynamic stability of a complex network whose elements are temporally updated through their interaction. Examples are found in biology, economics, sociology, and so on.

(ii) Weak chaos. Homeochaos suppresses strong chaos. The maximal Lyapunov exponent is positive, but is close to zero. The oscillation amplitude is not so large. This weak chaos, for example, is essential to avoid a too violent change or extinction in the population dynamics.

(iii) High-dimensional chaos. Homeochaos is high-dimensional chaos. There are many positive Lyapunov exponents, although their magnitude is small. The involved degrees of freedom is large.

The above three features are strongly interrelated. The stability is attained by the suppression of strong instability given by (ii). By (iii), strong chaotic instability is shared by many modes, implying the weak chaos per degrees of freedom (point (ii)).

The notion of homeochaos is independently discussed by Tsuda in the studies of neural dynamics[#9], where the point (i) is stressed as a functional possibility of chaos. The point (ii) (elimination of strong chaos) reminds us of the phrase "adaptation towards the *edge of chaos*" by Packard [22]. He has pointed out the importance of weak chaos in the biological information processing. In some examples of "edge of chaos", the degrees of freedom there may be rather high, implying that such state can be an illustration of homeochaos.

7. Flat versus rugged landscape

How does our scenario of a homeochaotic symbionet depend on the landscape? As has been seen in the previous sections, the valley height of fitness landscape is rather important. Here we summarize results for a flat landscape (neutral evolution), to see the role of landscape.

In a flat landscape ($\gamma = 0$ in our model), a state with a high mutation rate is more easily attained. As has already been shown in fig. 3, the transition is not sharp, and the resulting mutation level smoothly changes with coupling parameters.

Mutation in a flat landscape leads to free Brownian motion within all possible binary sequences. All species are easily connected through a single-point mutation, to form a large network. Thus the final cluster size is almost 2^k. There is no threshold for percolation for the coupling. The mutation level increases gradually with the coupling (see fig. 3). Temporally, the cluster size shows a transition to 2^k with the increase to a high mutation rate, and it is sustained at the large value later on. Since the whole

[#8]The importance of homeodynamics is discussed as *homeokinesis* by Iberall.

[#9]Tsuda has also proposed the notion of homeochaos in relation with neural dynamics [21].

connected species adjust the population depending on the parasite populations, the oscillation of each species is not strong. Its Lyapunov exponent is highly concentrated on a small positive value. The motion shows very weak chaotic oscillation. Number of positive exponents is very large, meaning high-dimensional weak chaos.

In a flat landscape, the distribution of average mutation levels is quite sharp. Even in a very strong coupling, where the mutation levels fluctuate with time, their averages are almost identical by species. There is no splitting of species into distinct mutation levels as is seen in a rugged landscape.

Even though the fitness is same for the whole species, the phase of oscillation is different by species. Some species oscillate in phase, others do out of phase (see fig. 4d). The species show spontaneous clustering into a few set of species by the phases of oscillations. Clustering may be a common feature in a nonlinear system with a global coupling [23]. In our model, there are a global coupling and a connection by mutation organized in a binary network. The latter connection may bring about a novel feature of clusterings, different from the previous studies [23].

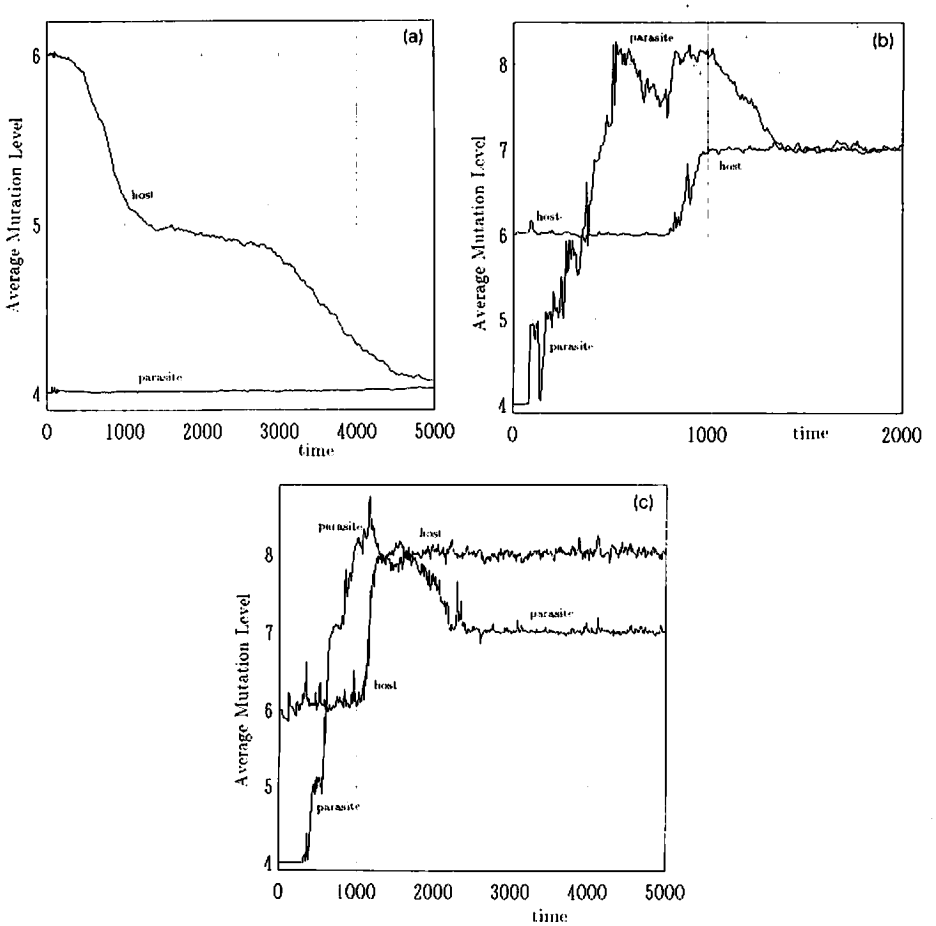

Fig. 13. Temporal change of average mutation levels of hosts and parasites: $g_0 = 0.001$, $g_h = 0.0001$, $E_0 = 0.4$, $\gamma = 0$. Initial species are 19 and 39 with mutation level 6 (for hosts) and 4 (for parasites). The bit sequence $k = 6$. (a) $c_h = 0.001$ and $c_p = 0.01$. (b) $c_h = 0.005$ and $c_p = 0.01$. (c) $c_h = 0.007$ and $c_p = 0.01$.

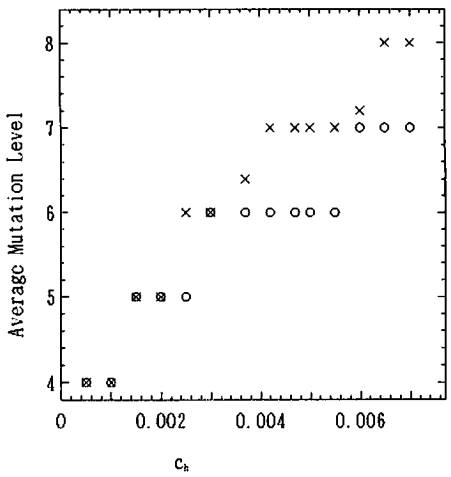

Fig. 14. Mutation level as a function of coupling c_h. Other parameters than c_h are the same as fig. 13.

8. Intrinsic formation of sustained high mutation rates

One might assume that the sustained high mutation rate is possible only if the mutation of either host or parasite is extrinsically set at a non-zero constant, to avoid its decreasing[#10]. This is not true.

We have simulated a model with mutation rates variable both for hosts and parasites. Here we treat only with the neutral landscape[#11]. Temporal changes of mutation levels are shown in fig. 13, while the dependence of final mutation levels on the coupling c_h is given in fig. 14. Again, both of the mutation rates are sustained at high levels, if the coupling of the interaction is large. The mutation rates for parasites and hosts are not necessarily identical. The average mutation levels again increase with the coupling in a stepwise manner.

As for the dynamics, we note that the increase of mutation rates of parasites precedes those of host species (see fig. 13). After this transient, the mutation level of hosts follows (and exceeds), while the level of parasites decreases till both the levels settle down to finite average levels.

The formation of oscillatory behaviors of symbionet is again observed essentially in the same manner as in the previous case. The oscillations of hosts and parasites are weakly chaotic. Initial large-amplitude oscillation is again eliminated through the evolution of mutation rates.

9. Summary and discussion

We have studied the evolution of mutation rate, by introducing a population model with mutation and interaction among species. In particular, we have simulated a model with interaction among hosts and parasites. Each species is coded by a bit sequence, and its fitness has a rugged or flat (neutral) landscape. The interaction is assumed to depend on the Hamming distance between the bit sequences of hosts and parasites.

[#10] We have also simulated a model with a variable mutation rate for parasites and a fixed one for hosts. Again, we have found a sustained high mutation rate with symbionet, consistent with other results throughout the present paper. As the coupling is increased, mutation rates of parasites increase, to form a connected network.

[#11] Throughout only this section we take the bit length $k = 6$.

First we note that the mutation rate is initially enhanced and then is lowered in a rugged landscape if there is no host–parasite interaction. This observation opens a possibility of automatic simulated annealing.

When the interaction between hosts and parasites is introduced, the mutation rate of hosts can be sustained at a high level. This sustained level depends on the coupling between hosts and parasites. If the landscape is rugged, the level goes up quite abruptly, as the coupling exceeds a threshold. This increase is percolative in nature. Indeed, a large cluster of species, connected by mutation, is formed through a sustained high mutation rate. This formation of symbionet is a key to resolve the paradox in mutation of mutation rates; paradox of the stability of a rule to change itself. As a level of each species, it is a paradox that a rule to change itself does not change to a rule not to change itself, i.e., a low (vanishing) mutation rate. In the level of ensemble of species, however, changing a rule to reproduce each species is no more paradox. All species live together in a network to keep their population with some mutational changes among species.

Note that the network is dynamically sustained. Population of each species oscillates chaotically in time. This is in contrast with previous arguments on the instability of a fixed point in a complex network. The oscillation is high-dimensional chaos with small positive Lyapunov exponents. If the mutation rate were zero, dynamics of each species would be essentially disconnected. Then some host–parasite pairs would show strong chaos, while some others would show periodic or fixed point dynamics. By sustaining a high mutation rate, chaotic instability is shared by almost all species, leading to weak high-dimensional chaos. This dynamic stability with high-dimensional chaos is termed "homeochaos".

When the fitness is neutral, mutation rates are more easily sustained at a finite level. The final mutation level increases gradually with the coupling. Although the fitness is same for all species, there appears spontaneous differentiation. Oscillations of population are not synchronized, but have some clustering of phases.

These results also hold even if we assume that the mutation rate of parasites can also mutate. Both the mutation rates of hosts and parasites are sustained at a high level, again depending on coupling of the interaction of hosts and parasites.

The behaviors presented through the paper are generally observed in our model with a wide range of parameters and initial conditions, as long as the whole species of hosts and/or parasites are not extinct. With the increase of couplings, we have always seen the percolative increase of mutation rates in a rugged landscape. Thus we believe that our maintenance of mutation rates through the self-organization of homeochaotic symbionet is general in an evolutionary system with interaction among species.

Formation of network from a level of individuals is important in various fields in biological science. Let us briefly survey possible relevance of our results to biological networks.

(1) Autocatalytic network: This problem is studied in relation with the problem of origin of life [24]. Although the percolative aspect is similar to ours, their model leads to a fixed-point type solution. There is no prey–predator-type interaction which leads to the oscillation in our case. Our model belongs to a different class from their studies.

(2) Immune network: antibody–antigen interactions are essentially of the same type with our host–parasite interaction. An antigen is damaged by "matched" antibodies. An antibody is again damaged by a specific class of antibodies. Jerne [25] proposed a formation of antibody–antigen network. Percolative formation of networks is found in a model simulation of bit string matching [26]. In an immune system, we note a very high mutation rate for antibodies. Oscillation of antibody concentration and immune activities is also discovered. These features are common with our formation of symbionet with a high mutation rate. If our symbionet is valid to the immune network, it provides a possible

mechanism of the existing high mutation rate in the immune system. We also expect that the population of antibody species may exhibit a homeochaotic oscillation. Of course, our model is not realistic enough to allow for detailed comparison with an immune system, and it is an important future problem to extend our model by including antibody–antibody interaction and ring formation of antibodies [27], and so on.

Another interesting problem in a somatic evolution is the formation and maintenance of a society of differentiated cells [28], as is also important in the origin of multicellular organism. By cell division, each cell reproduces itself with differentiation and possible mutational changes. Symbiotic cell society is formed from self-reproducing cells, as is similar to our formation of symbionet. Although dynamical aspects are rather different between the two, and the interaction among cells is much more complicated than our host–parasite interaction, it is interesting in future to construct a simple model for cell society, starting from our viewpoint of symbionet.

(3) Ecological network: Of course, our model is originated in the ecological network. The importance of symbiosis with many species is stressed by Margulis and Lovelock [29]. Prey–predator-type interaction is common in the ecology. Then, can we find a homeochaotic symbionet there? We believe so. The stability of a complex ecological system is only sustained dynamically. A fixed point or a periodic state for many species is usually unstable [19]. A typical example of complex ecological network is seen in the species in rain forest. The ecological dynamical system of rain forest has following features [30][#12]: (i) there are a huge number of species; (ii) populations of some species are very few; (iii) temporal variation of population of each species is rather large; dominant species may change in time, and extinction and appearance of new species seem to be more frequent than in the temperate zones. Indeed, features (i)–(iii) are also seen in our homeochaotic symbionet in a strong coupling regime. If our argument is relevant to the dynamics in rain forest, it is important to confirm the feature (iii) from real data and to check the dynamical change of each species, which, we believe, is homeochaotic. We also hope the observation of the mutation rate itself, which we may expect to be larger than the normal level. If this is the case, we may assume that the coupling among species is effectively larger than in the temperate zones.

(4) Neural net: The Darwinian viewpoints have been presented in the evolutionary epistemology. In the studies of neural dynamics, the idea of evolution with selectivity and variation is emphasized by Edelman [31]. In Edelman's neural Darwinism, neuronal groups are under selective pressure at a somatic level. "Mutation" comes from synaptic plasticity. So far, interactions among neuronal groups are not fully considered. If we introduce our idea of mutation of mutation rates to neural Darwinism, it may be possible to change a rule of synapticity itself, through, for example, control of chemical concentration. In a psychological level, this "plasticity of plasticity" may be related with the learning of "how-to-learn".

(5) Complex adaptive systems in general: Our model provides a prototype dynamics for a network system such that (i) the number of involved units is large, (ii) the dynamics of variables attached to the units (e.g., population) depends on the mutual interaction and that (iii) the dynamics itself can change in time following some inherent dynamics (e.g. mutation of mutation rates in our case). Indeed, such network systems are generally seen in a wide-ranged field in biology, sociology, economics, computer science, and the engineering. We believe that our formation of symbionet through homeochaos is a common feature for such network systems. The dynamic stability is attained with cooperation of individual units, in many existing network systems such as social networks, the economics of interacting many agents, the ecology of computer networks, and chemical network in our body. Our homeochaos

[#12] Connell [30] discusses the fact that the diversity in tropical rain forests are maintained only in a nonequilibrium state. Our homeochaotic state provides such maintenance of a non-equilibrium state.

provides the key principle for the formation of the cooperation and the dynamic stability required in such systems.

For long time homeostasis was thought to be an essential mechanism for the survival of organisms in the fluctuating environment. Recently, the importance of oscillatory behavior has been appreciated in most fields in biology. Stability of a biological system is not sustained in a fixed point, but in a dynamical state. In our example, formation of weak high-dimensional chaos is essential to keep a system away from extinction. Population in our model is sustained not at a static state, but through *homeochaos*. There, too violent change is removed through high-dimensional dynamics. This elimination of strong low-dimensional chaos may be one possible reason for the absence of low-dimensional chaos in a wild ecological system [32]. We believe that homeochaos is essential to keep the dynamical stability of complex biological networks in general.

Acknowledgements

The authors would like to thank Kensuke Ikeda, Ichiro Tsuda, Yoshitsugu Oono, Peter Davis, and Walter Fontana for exciting discussions and critical comments. This study is carried out as a cooperative research program at Yukawa Institute of Fundamental Physics. It is also partially supported by Grants-in-Aid for Scientific Research from the Ministry of Education, Science, and Culture of Japan.

Appendix. Evaluation of eigenvalues

In this appendix, we evaluate the stability for the fixed point of our dynamics (1) and (2). The Jacobi matrix for eqs. (1) and (2) is given by

$$\begin{pmatrix} D_{11} & D_{12} & D_{13} & \cdot \\ D_{21} & D_{22} & \cdot & \cdot \\ D_{31} & \cdot & \cdot & \cdot \\ \cdot & \cdot & \cdot & \cdot \end{pmatrix}, \quad D_{ij} = \begin{vmatrix} \dfrac{1}{1+g_p p_i^*} & \dfrac{c_p p_i^*}{1+g_p p_i^*} \\ \dfrac{-c_h h_i^*}{1+g_h \Sigma h_i^*} & 1 - \dfrac{g_h h_i^*}{1+g_h \Sigma h_i^*} \end{vmatrix} \delta_{ij}$$

at the fixed point (p_i^*, h_i^*). The fixed points have the following forms:

$$p(i)^* = \frac{(\langle\alpha\rangle - 1)c_p - (1-d)g_h'}{c_p c_h + g_p g_h'} + \frac{\alpha(i) - \langle\alpha\rangle}{c_h}$$

and

$$h(i)^* = \frac{(\langle\alpha\rangle - 1)g_p + (1-d)c_h}{c_p c_h + g_p g_h'} + \frac{g_p(\alpha(i) - \langle\alpha\rangle)}{c_h c_p},$$

where $\langle\alpha\rangle = \Sigma_i \exp[E_0 - E(i)]/\Sigma_i 1$ and $g_h' = g_h \Sigma_i 1$.

In order to get the analytical form of the eigenvalues, the following approximated matrix is studied:

$$D_{ij} = \begin{vmatrix} 1 - g_p p_i^* & c_p p_i^* \\ -c_h p_i^* & 1 \end{vmatrix} \delta_{ij} + \mathcal{O}\left(g_p^2, g_h\right).$$

For the neutral landscape, eigenvalue λ is shown to satisfy the relation

$$(\operatorname{Im}\lambda)^2 + \left(\frac{c_p + 4g_h'}{c_p}\right)\left(\operatorname{Re}\lambda - 1 + \frac{c_p(\langle\alpha\rangle - 1) - 2g_h'(1-d)}{c_p + 4g_h'}\right)^2 = \Omega^2,$$

where $\Omega^2 = [c_p(\alpha - 1)(\alpha - d) - (1-d)^2 g_h']/c_p + 4g_h'$. When $|\lambda|$ exceeds 1, a Hopf bifurcation to periodic oscillation sets in, with the emergence of chaotic oscillation through the further increase of couplings. Stability condition for the fixed point is given by $|\lambda| < 1$, in terms of c_h:

$$c_h > g_p(2 - \langle\alpha\rangle)/2(1-d)\left[1 + \sqrt{1 + 4(1-d)g_h'/c_p(2 - \langle\alpha\rangle)^2}\right].$$

The critical value of c_h breaking the linear stability is estimated as $c_h \approx 0.053$ under typical parameter values of our simulation ($g_h' = g_p = 0.01$, $c_p = c_h = 0.01$, $<\alpha \approx 1.7$, $d = 0.9$). This value is approximately coincident with the observed value. If the ruggedness of the landscape is not large ($\alpha(i) - \langle\alpha\rangle \ll 1$), essentially the same condition is obtained for the stability.

References

[1] See, e.g., J.W. Drake, The Molecular Basis of Mutation (Holden-Day, San Francisco, 1970).
[2] E.C. Friedberg, DNA Repair (Freeman, San Francisco, 1985).
[3] W.D. Hamilton, R. Axelrod and R. Tanase, Proc. Nat. Acad. Sci. 87 (1990) 3566.
[4] K. Ishii, H. Matsuda, Y. Iwasa and A. Sasaki, Genetics 121 (1989) 163.
[5] J. Holland, in: Escaping Brittleness in Machine Learning II, eds. R.S. Mishalski, J.G. Carbonell and T.M. Miechell (Kaufman, 1986).
[6] See, e.g., S. Kim, M. Davis, E. Sinn, P. Patten and L. Hood, Cell 25 (1981) 59;
L. Wysocki, T. Manser and M.L. Gefter, Proc. Nat. Acad. Sci. USA 83 (1986) 1847.
[7] K. Rajewsky, private communication.
[8] K. Gödel, Mon. Math. Phys. 38 (1931) 173;
E. Nagel and J.R. Newman, Gödel's proof (New York Univ. Press, New York, 1958).
[9] D.R. Hofstadter, Gödel, Escher, Bach (Basic Books, 1979).
[10] L. Margulis, Symbiosis in Cell Evolution (Freeman, San Francisco, 1981).
[11] T. Ikegami and K. Kaneko, Physica D42 (1990) 235.
[12] M. Kimura, The Neutral Theory of Molecular Evolution (Cambridge Univ. Press, Cambridge, 1983).
[13] S.A. Kaufmann and S. Levin, J. Theor. Biol. 128 (1987) 11.
[14] M. Mezard, G. Parisi and M.A. Virasoro eds., Spin Glass Theory and Beyond (World Scientific, Singapore, 1988).
[15] P.W. Anderson, Proc. Nat. Acad. Sci. USA 80 (1983) 3386.
[16] T. Ikegami and K. Kaneko, Phys. Rev. Lett. 65 (199) 3352.
[17] S. Kirkpatrick, C.D. Gellat and M.P. Vecchi, Science 220 (1983) 671.
[18] T. Ikegami and K. Kaneko, Automatic simulated annealing by mutation of mutation rates, in preparation (1992).
[19] R. May, Stability and Complexity in Model Ecosystems (Princeton Univ. Press, Princeton, 1973).
[20] A.S. Iberall, Am. J. Physiol. 223 (1978) 171;
F.E. Yates, Am. J. Physiol. 238 (1980) 277.
[21] I. Tsuda, Chaotic itinerancy as a dynamical basis of hermeneutic process in brain and mind, World Future 32 (1991) 167.

[22] N.H. Packard, in: Dynamic Patterns in Complex Systems, eds. J. Kelso, A.J. Mandell and M.F. Shlesinger (World Scientific, Singapore, 1988) pp. 293–301.
[23] K. Kaneko, Phys. Rev. Lett. 63 (1989) 219; Physica D 41 (1990) 137.
[24] J.D. Farmer, S.A. Kauffman and N.H. Packard, Physica D 22 (1986) 50.
[25] N.K. Jerne, in The neurosciences: A study program, eds. G.C. Quarton, T. Melnechuk, and F.O. Schmitt, Rockefeller Univ. Press.
[25] J.D. Farmer, N.H. Packard and A. Perelson, Physica D 22 (1986) 187.
[27] T. Ikegami, Ph. D. Thesis (1989);
T. Ikegami and K. Kaneko, to be published.
[28] L.W. Buss, The evolution of individuality (Princeton Univ. Press, Princeton, 1987).
[29] J. Lovelock, Gaia: A New Look at Life on Earth (Oxford Univ. Press, Oxford, 1979);
L. Margulis and D. Sagan, Microcosmos (Summit Books, 1986).
[30] J. Kikkawa, Kagaku 60 (1990) 603 (in Japanese);
J.H. Connel, Science 199 (1978) 1302.
[31] G.M. Edelman, Neural Darwinism (Basic Books, 1987).
[32] R. May, Nature 26 (1976) 459.